Lumped Capacitance and Open End Effects of Striplike Structures in Multilayered and Anisotropic Substrates

RAFAEL R. BOIX AND MANUEL HORNO, MEMBER, IEEE

Abstract—**Variational techniques in the spectral domain are used to calculate the lumped capacitance of a rectangular patch embedded in an arbitrary multilayered anisotropic substrate in a very accurate way. The results obtained are applied to the determination of the quasi-static edge capacitance of semi-infinite striplines and microstrip lines.**

I. Introduction

PLANAR MICROSTRIP structures consisting of transmission lines, discontinuities, and lumped elements are nowadays widely used in MIC's and MMIC's. In the case of finite-sized elements, rectangular and circular patches are used as capacitors. Another subject of interest is that of discontinuities, which invariably appear in any microstrip circuit. When discontinuity dimensions are much smaller than the wavelength, they may be approximated by lumped-element equivalent circuits. For instance, an *RLC* termination can be used as a model for an abruptly ended microstrip. In fact, in this case it is only necessary to take into account the capacitive effect because it turns out to be dominant when frequencies are kept below the quasi-static limit [1],[2].

In this paper, we focus our attention on the calculation of the lumped capacitance of a rectangular patch and the edge capacitance of an open-circuit striplike line, both embedded on a stratified substrate consisting of anisotropic lossless dielectric layers. Multilayered structures are included because they are used in MMIC applications when several metal layers are involved. The effect of anisotropy is also studied because significant errors may be incurred when it is neglected in analyzing uniaxial and biaxial substrates [3],[4]. In fact, extensive work on the characterization of infinite planar transmission lines on anisotropic substrates can be found in the existing literature [3], but the influence of anisotropy on the design of lumped elements and discontinuities has hardly been studied [5]. In the analysis, variational techniques in the spectral domain are used [6],[7] since they present inherent advantages over other reported methods in the spatial domain [8],[9]. Design graphs which enhance and generalize previously reported results are given.

Manuscript received November 1, 1988; revised March 27, 1989. This work was supported by the C.I.C.Y.T. under Project PB86-0144.

The authors are with the Department of Electronics and Electromagnetics, Faculty of Physics, University of Seville, 41012 Seville, Spain.

IEEE Log Number 8929893.

II. Outline of the Theoretical Procedures

In Fig. 1(a) is shown the cross section of a stratified medium composed of N layers of lossless, anisotropic, dielectric materials. Either one rectangular conductor plate (Fig. 1(b)) or one semi-infinite conductor strip (Fig. 1(c)) is placed at the Mth interface of the multilayered structure, both referred to the coordinate axes as it is shown in Fig. 1(a)–(c). The conductors are assumed to be lossless and infinitely thin. The interfaces $i=0$ and $i=N$, which limit the multilayered structure, are allowed to be any of three possibilities: electric walls, magnetic walls, or open boundaries. In the analysis of the rectangular plate shown in Fig. 1(b), each dielectric is defined by a general symmetric permittivity tensor, given by the following expression:

$$\bar{\epsilon}_i = \epsilon_0 \begin{bmatrix} \epsilon^*_{11,i} & \epsilon^*_{12,i} & \epsilon^*_{13,i} \\ \epsilon^*_{12,i} & \epsilon^*_{22,i} & \epsilon^*_{23,i} \\ \epsilon^*_{13,i} & \epsilon^*_{23,i} & \epsilon^*_{33,i} \end{bmatrix} \qquad (i=1,\cdots,N). \quad (1)$$

The elements of tensor $\bar{\epsilon}_i$ can be expressed as a function of its eigenvalues ϵ_{xi}, ϵ_{yi}, and ϵ_{zi} and of the Euler angles ϕ_i, θ_i, and ψ_i, which describe the position of its principal axes referred to the coordinate axes chosen in Fig. 1(a). When we study the open-circuit striplike line (Fig. 1(c)), we restrict ourselves to dielectric substrates with uniaxial anisotropy and tilted optical axis in the $X-Y$ plane of Fig. 1(a). Therefore, in that case, the tensor $\bar{\epsilon}_i$ in (1) is such that $\epsilon^*_{13,i} = \epsilon_{23,i} = 0$ $(i=1,\cdots,N)$.

It is possible to find a variational expression in the spectral domain for the capacitance of the rectangular plate of Fig. 1(b) embedded in the multilayered structure of Fig. 1(a). This expression can be written as [7]

$$1/C = (1/4\pi^2 Q^2)\int_{-\infty}^{+\infty}\int_{-\infty}^{+\infty} G(\alpha,\beta)|\rho(\alpha,\beta)|^2\, d\alpha\, d\beta. \quad (2)$$

Here, $\rho(\alpha,\beta)$ is the two-dimensional Fourier transform of the charge density on the plate in the $X-Z$ plane and $G(\alpha,\beta)$ may be interpreted as the Fourier transform of the Green's function worked out at the interface on which conductors lie [6]. Following Thomson's theorem, (2) provides a lower bound of the capacitance.

0018-9480/89/1000-1523$01.00

Since the previous expression is stationary, a good approximation of the charge density on the conductor plate may yield a very accurate value of the capacitance. To optimize the results, trial function expansions are used to represent the charge density. The Rayleigh–Ritz method is applied to determine the unknown weighting coefficients. Trial functions should be chosen in such a way that they fulfill the physical constraints of the problem, such as the discontinuity that the charge density has at the edges of the conductor plate. In this sense, we enhance previous charge density approximations [6],[7] and we propose the following expression:

$$\rho(x,z) = f(x)g(z) \tag{3}$$

where

$$f(x) = \left\{ (2/\pi W)\left[1/\left(1-(2x/W)^2\right)\right]^{1/2} + (2/\pi W)\sum_{i=1}^{n1} a_i T_{2i}(2x/W) \cdot \left[1/\left(1-(2x/W)^2\right)\right]^{1/2} \right\} \tag{4a}$$

and

$$g(z) = \left\{ (2/\pi L)\left[1/\left(1-(2z/L)^2\right)\right]^{1/2} + (2/\pi L)\sum_{j=1}^{n2} b_j T_{2j}(2z/L)\left[1/\left(1-(2z/L)^2\right)\right]^{1/2} \right\}. \tag{4b}$$

$T_{2i}(x)$ are Chebyshev polynomials of the first kind.

The spectral Green's function $G(\alpha,\beta)$ appearing in (2) can be analytically obtained. To achieve this, the recurrent algorithm developed by the authors in [10] has been extended to analyze three-dimensional geometries with general anisotropy. The details of the calculation of $G(\alpha,\beta)$ are explicitly given in Appendix I. From the expression of $G(\alpha,\beta)$, it can be inferred that a direct equivalence between isotropic and anisotropic substrates in three dimensions can only be made when we deal with uniaxial anisotropic substrates having the optical axis aligned with the Y axis appearing in Fig. 1(a). This is the particular case discussed in [5].

The capacitive fringe effect of a semi-infinite microstrip line (or stripline) is described by means of an open-circuit capacitance C_{oc}, which can be worked out as [7]

$$C_{oc} = 0.5 \lim_{L\to\infty} \left(C(L) - LC\right). \tag{5}$$

Here, $C(L)$ is the capacitance of a rectangular conductor patch in which the width is that of the strip and the length is L. C is the capacitance per unit length of a microstrip or stripline. This capacitance can be calculated with the techniques described in [10] for a multilayered and anisotropic substrate. It was proved that the expression in brackets appearing in (5) converges to a limit when L is taken to be between 10 and 20 times the distance between the rectangular conductor plate and the nearest ground plane. Calculating $C(L)$ usually means calculating the capacitance of a rectangular patch in which $L >> W$. For these narrow plates, the charge density along the longer direction remains nearly constant except for a region around the edge of the plate, in which it quickly grows, becoming discontinuous. The excess charge density is precisely the cause of the fringe capacitance of the open-circuit striplike line [1]. To account for the behavior of the charge density in narrow patches, the trial functions along the longer direction were chosen to be different from the ones defined in (4b). In those cases, the charge density dependence on the z coordinate is given by

$$g(z) = (1/L) + \sum_{j=1}^{n2} b_j \left\{ \left[1/H(L/2-z)\right]^{1/2} \cdot \exp\left(-j((L/2-z)/H)\right) + \left[1/H(L/2+z)\right]^{1/2} \exp\left(-j((L/2+z)/H)\right) - 2(\pi/j)^{1/2}(1/L) \right\} \tag{6}$$

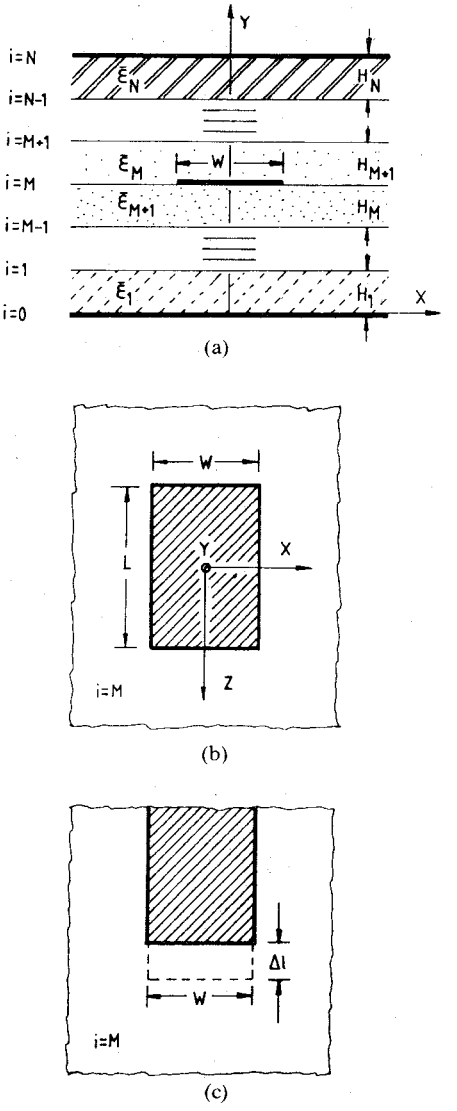

(a) (b) (c)

Fig. 1. (a) Anisotropic and multilayered substrate. (b) Rectangular conductor patch lying on the Mth interface of the multilayered substrate shown in (a). (c) Semi-infinite strip lying on the Mth interface of the multilayered substrate shown in (a).

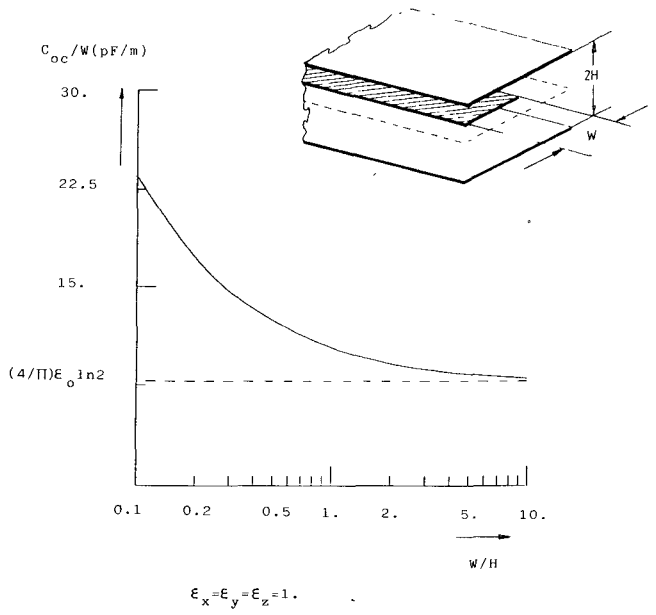

Fig. 2. Open-circuit capacitance of a stripline in vacuum. The dashed line indicates the edge capacitance per unit length of a semi-infinite plate between ground planes.

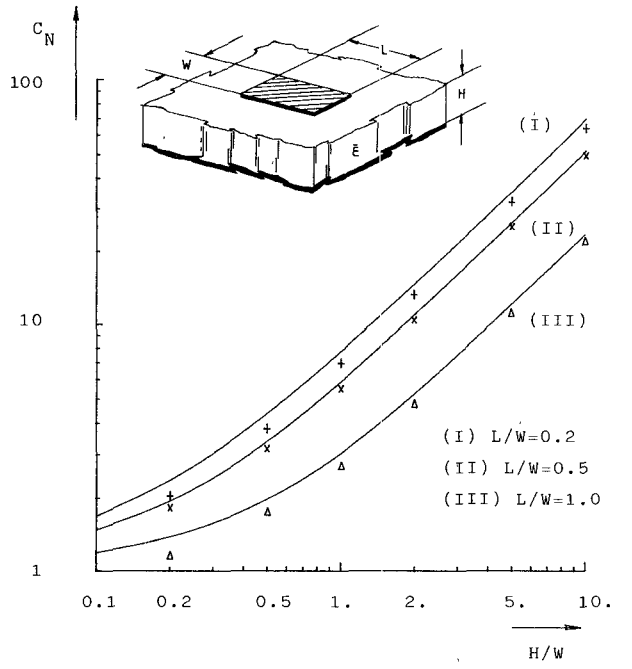

Fig. 3. Normalized capacitance ($C_N = CH/\epsilon_0 WL\epsilon_{22}^*$) of a rectangular conductor patch on isotropic and uniaxial anisotropic substrates: (I) ($\epsilon_x = \epsilon_y = \epsilon_z = 6.0$) Comparison with the results obtained in [6] (+). (II) Pyrolitic boron nitride [3] with aligned optical axis ($\epsilon_x = \epsilon_z = 5.12; \epsilon_y = 3.4$; $\phi = \theta = \psi = 0$). Comparison with Koul *et al.* [5] (x). (III) Sapphire [3] with aligned optical axis ($\epsilon_x = \epsilon_z = 9.4$; $\epsilon_y = 11.6$; $\phi = \theta = \psi = 0$). Comparison with [5] (Δ).

where

$$H = \min\left(\sum_{i=1}^{M} H_i, \sum_{i=M+1}^{N} H_i\right).$$

In Appendix II, we provide the expression of the charge density transform $\rho(\alpha, \beta)$ obtained when the functions defined in (4a), (4b), or (6) are introduced into (3).

It is necessary to point out that the determination of the capacitance by means of (2) requires the calculation of complicated double integrals all over the $\alpha-\beta$ plane. The CPU time involved in the direct process using Cartesian coordinates in the transformed plane can be very high. To avoid this, plane polar coordinates were used. Concerning the radial part of the integrals, the asymptotic behavior of the functions to be integrated was extrapolated and analytically integrated. Numerical integration was then carried out over the initial functions minus their asymptotic behavior. Once the radial integrals had been obtained, the angular integrals were calculated by using Gauss–Legendre quadratures. Thanks to these modifications, the integration process was considerably accelerated.

III. Results

In Fig. 2, the open-circuit capacitance per unit strip width of a stripline in vacuum is plotted versus the ratio W/H. As the strip width increases, the values of the open-circuit capacitance asymptotically tend to the value of the edge capacitance per unit length of a semi-infinite conductor plate between ground planes, which can be analytically obtained by conformal mapping.

In Fig. 3, the capacitance of square and rectangular microstrip patches is plotted as a function of the ratio W/H. Graphs are presented for one isotropic substrate ($\epsilon = 6$) and for two uniaxial anisotropic substrates (sapphire and pyrolitic boron nitride) with optical axis perpendicular to the ground plane. The analysis of these three cases, which correspond to axially symmetric substrates, has already been carried out in the literature [5],[6]. Comparison is made with previously reported results and it can be seen that the percent agreement is not very close (in some cases, the difference reaches 10 percent or even more). The origin of the existing discrepancy between the results is believed to be the inaccurate charge density approximations chosen by the authors in the reported references. In [6], the charge density on the rectangular patch is taken to be constant. In [5], the charge density is approximated by using a third-degree polynomial in the X direction and a uniform distribution in the Z direction (see Fig. 1(b)).

In Fig. 4, we present graphs for the capacitance of rectangular patches on uniaxial anisotropic substrates with tilted optical axis. In this case, the substrates no longer present axial symmetry and the analysis performed in [5] cannot be applied.

In Fig. 5, the edge capacitance of an open circuit on isotropic and anisotropic substrates is plotted versus W/H. In the isotropic case, we compare our results with those reported by Silvester *et al.* [1]. These authors employ a polynomial expansion to approximate the bidimensional charge density excess at the edge of the open-circuit microstrip. Therefore, they also omit the edge singularity of the charge density in their calculations. Owing to this, some disagreement is found between their results and ours.

In Fig. 6, the effect of biaxial anisotropy on the capacitance of a rectangular patch is studied. The angles between the principal axes of the permittivity tensor and the coor-

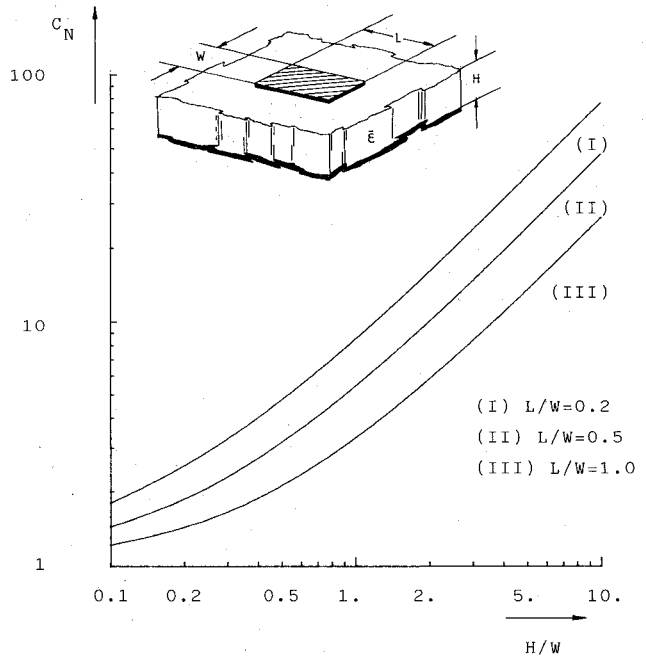

Fig. 4. Normalized capacitance ($C_N = CH/\epsilon_0 WL\epsilon_{22}^*$) of rectangular conductor patch on uniaxial anisotropic substrates with tilted optical axis in the $X-Y$ plane: (I) Anisotropic Kapton [4] ($\epsilon_x = \epsilon_z = 3.0$; $\epsilon_y = 3.5$; $\theta = \pi/4$; $\phi = \psi = 0$). (II) Pyrolitic boron nitride ($\epsilon_x = \epsilon_z = 5.12$; $\epsilon_y = 3.4$; $\theta = \pi/6$; $\phi = \psi = 0$). (III) Sapphire ($\epsilon_x = \epsilon_z = 9.4$; $\epsilon_y = 11.6$; $\theta = \pi/3$; $\phi = \psi = 0$).

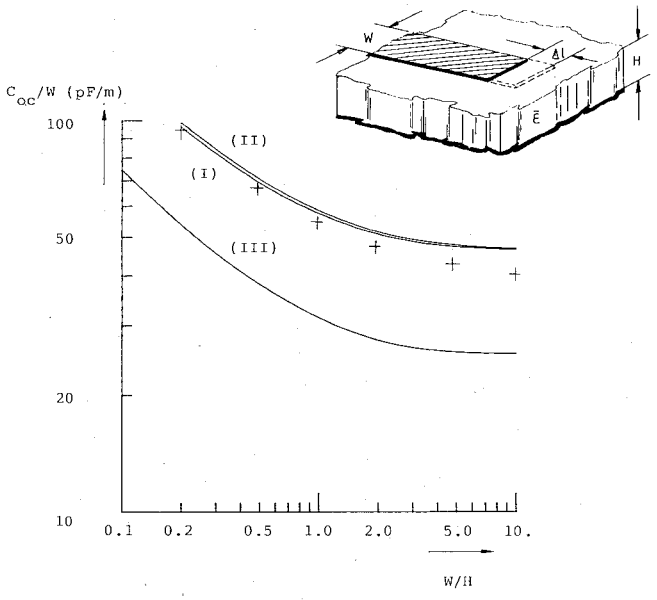

Fig. 5. Open-circuit capacitance of an abruptly ended microstrip: (I) ($\epsilon_x = \epsilon_y = \epsilon_z = 9.6$). Comparison with the results appearing in [1] (+). (II) Sapphire with tilted optical axis ($\theta = \pi/3$). (III) Pyrolitic boron nitride with tilted optical axis ($\theta = \pi/6$).

dinate axes are separately allowed to vary over the three coordinate planes.

Finally, in Fig. 7, the effect of an isotropic inhomogeneous substrate with a varying permittivity in the Y direction on the edge capacitance of an open-circuit stripline is analyzed. To simulate the varying permittivity, the substrate has been divided into 20 layers of constant permittivity. The permittivity of each layer is taken to be equal to the value of $\epsilon(y)$ in the middle point of the layer.

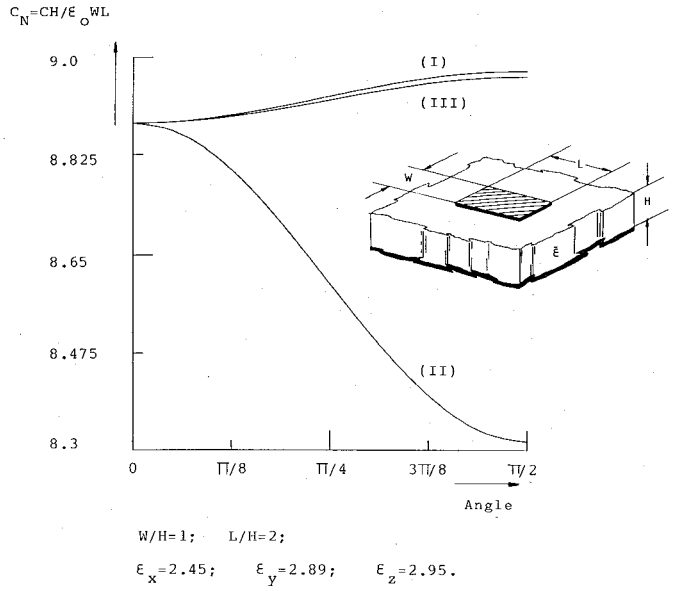

Fig. 6. Normalized capacitance ($C_N = CH/\epsilon_0 WL$) of a rectangular patch as a function of the tilting angle between the principal axes of the permittivity tensor and the coordinate axes defined in Fig. 1(b) for a biaxial substrate of PTFE [4]: (I) Tilt in $X-Z$ plane ($\theta = \psi = 0$). (II) Tilt in $X-Y$ plane ($\phi = \psi = 0$). (III) Tilt in $Y-Z$ plane ($\phi = \psi = \pi/2$).

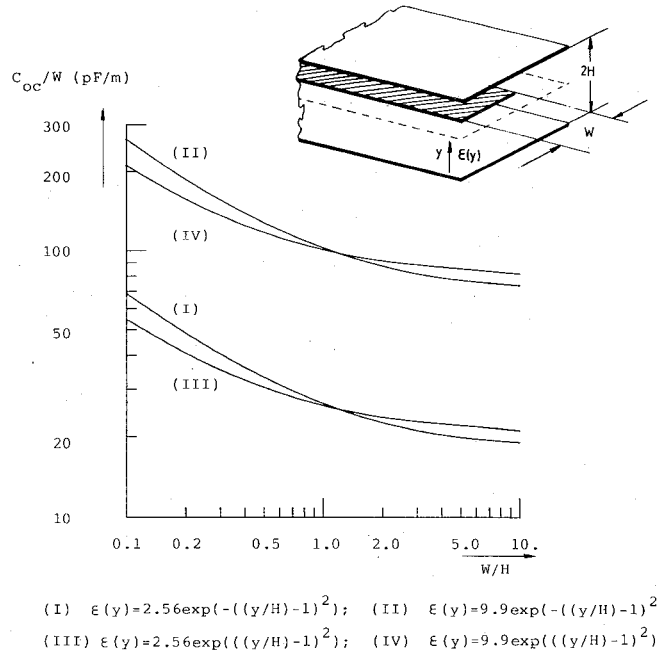

Fig. 7. Edge capacitance of a stripline filled with an isotropic substrate with a varying permittivity in the Y direction: (I), (II) Gaussian distribution. (III), (IV) Inverted Gaussian distribution.

IV. Conclusions

An accurate calculation of the lumped capacitance of a rectangular microstrip patch and the edge capacitance of an open-circuit microstrip or stripline is carried out. Variational expressions in the spectral domain are developed to analyze these conductors when they are embedded in a

multilayered anisotropic substrate. A recurrence algorithm, easy to compute, is proposed to determine the three-dimensional spectral Green's function characterizing the sort of substrates employed. The method makes it possible to study biaxial substrates in the case of the rectangular patch and uniaxial substrates with tilted optical axis in the transverse plane in the case of open-circuit striplike transmission lines. A detailed study of trial functions to approximate the charge density on the conductors is carried out, taking into account the physical features of each problem. The results obtained are compared with those appearing in the literature. Original design graphs are presented, with special emphasis on the use of inhomogeneous and anisotropic substrates.

Appendix I

The algorithm developed to calculate the spectral Green's functions associated with three-dimensional problems involving multilayered and anisotropic substrates basically presents the same recurrence relations reported in [10] and [11]. However, certain expressions need to be redefined owing to the fact that in this case, we deal with three-dimensional physical structures and two-dimensional Fourier transforms.This is the case with the coefficients $\tilde{g}_{i+1,i}$ and $\tilde{g}_{i,i}$ $(i=1,\cdots,N-1)$, defined in [10] and [11], which are now given by

$$\tilde{g}_{i+1,i}(\alpha,\beta) = -\epsilon_0 F_{i+1}\epsilon^*_{22,i+1}\exp(-jQ_{i+1}H_{i+1}) \cdot [\sinh(F_{i+1}H_{i+1})]^{-1} \quad (7)$$

$$\tilde{g}_{i,i}(\alpha,\beta) = \epsilon_0\left[\epsilon^*_{22,i}F_i\coth(F_iH_i) + \epsilon^*_{22,i+1}F_{i+1}\coth(F_{i+1}H_{i+1})\right] \quad (8)$$

where $Q_i(\alpha,\beta)$ and F_i (α,β) are functions of the spectral variables α and β, which can be written as

$$Q_i(\alpha,\beta) = (\alpha\epsilon^*_{12,i} + \beta\epsilon^*_{23,i})/\epsilon^*_{22,i} \quad (9)$$

$$F_i(\alpha,\beta) = (1/\epsilon^*_{22,i})\left[\alpha^2\left(\epsilon^*_{11,i}\epsilon^*_{22,i} - (\epsilon^*_{12,i})^2\right) + \beta^2\left(\epsilon^*_{22,i}\epsilon^*_{33,i} - (\epsilon^*_{23,i})^2\right) + 2\alpha\beta(\epsilon^*_{13,i}\epsilon^*_{22,i} - \epsilon^*_{12,i}\epsilon^*_{23,i})\right]^{1/2} \quad (i=1,\cdots,N). \quad (10)$$

Once these changes are carried out, the rest of the algorithm described in [11] remains valid for our purposes.

Appendix II

According to (3), the charge density transform $\rho(\alpha,\beta)$ can be expressed as

$$\rho(\alpha,\beta) = \int_{-(W/2)}^{+(W/2)} f(x)e^{-j\alpha x}\,dx \int_{-(L/2)}^{+(L/2)} g(z)e^{-j\beta z}\,dz = f(\alpha)g(\beta). \quad (11)$$

Following (4a), $f(\alpha)$ is given by

$$f(\alpha) = J_0(\alpha W/2) + \sum_{i=1}^{n1} a_i(-1)^i J_{2i}(\alpha W/2) \quad (12)$$

where $J_{2i}(x)$ are Bessel functions of the first kind.

In the case of rectangular plates with average dimensions, (4b) is used for $g(z)$, and in this case $g(\beta)$ can be written

$$g(\beta) = J_0(\beta L/2) + \sum_{j=1}^{n2} b_j(-1)^j J_{2j}(\beta L/2). \quad (13a)$$

For narrow rectangular plates, (6) must be used for $g(z)$; in this case $g(\beta)$ is given by

$$g(\beta) = (2/\beta L)\sin(\beta L/2) + \sum_{j=1}^{n2} b_j\left\{\left[(2\sqrt{\pi})/\left(j^2+(\beta H)^2\right)^{1/4}\right] \cdot \cos\left[(1/2)(\beta L - \arctan(\beta H/j))\right] - 2(\pi/j)^{1/2}(2/\beta L)\sin(\beta L/2)\right\}. \quad (13b)$$

To derive this last expression, we have employed the fact that $\exp(-(jL/H)) \approx 0$ when $L/H \geq 10$ $(j=1,\cdots,n2)$. That means that (13b) is valid as long as $L/H \geq 10$. For practical purposes, this is not a difficulty since the value of L needed to calculate C_{oc} in (5) can be as high as we wish.

References

[1] P. Silvester and P. Benedek, "Equivalent capacitances of microstrip open circuits," *IEEE Trans. Microwave Theory Tech.*, vol. MTT-20, pp. 511–516, Aug. 1972.

[2] R. Troughton, "Design of complex microstrip circuits by measurement and computer modelling," *Proc. Inst. Elec. Eng.*, vol. 118, no. 3/4, pp. 469–474, Mar./Apr. 1971.

[3] N. G. Alexópoulos, "Integrated-circuit structures on anisotropic substrates," *IEEE Trans. Microwave Theory Tech.*, vol. MTT-33, pp. 847–881, Oct. 1985.

[4] H. Yang and N. G. Alexópoulos, "Uniaxial and biaxial substrate effects on finline characteristics," *IEEE Trans. Microwave Theory Tech.*, vol. MTT-35, pp. 24–29, Jan. 1987.

[5] S. K. Koul and B. Bhat, "Evaluation of end effects and lumped capacitance of microstrip with anisotropic substrates," in *Proc. 15th European Microwave Conf.*, 1985, pp. 148-153.

[6] Y. Rahmat-Samii, T. Itoh, and R. Mittra, "A spectral domain analysis for solving microstrip discontinuity problems," *IEEE Trans. Microwave Theory Tech.*, vol. MTT-22, pp. 372–378, Apr. 1974.

[7] B. Bhat and S. K. Koul, "Lumped capacitance, open-circuit end effects, and edge capacitance of microstrip-like transmission lines for microwave and millimeter-wave applications," *IEEE Trans. Microwave Theory Tech.*, vol. MTT-32, pp. 433–439, Apr. 1984.

[8] A. Farrar and A. T. Adams, "Matrix methods for microstrip three-dimensional problems," *IEEE Trans. Microwave Theory Tech.*, vol. MTT-20, pp. 497–504, Aug 1972.

[9] P. Benedek and P. Silvester, "Capacitance of parallel rectangular plates separated by a dielectric sheet," *IEEE Trans. Microwave Theory Tech.*, vol. MTT-20, pp. 504–510, Aug. 1972.

[10] R. R. Boix and M. Horno, "Modal quasistatic parameters for coplanar multiconductor structures in multilayered substrates with arbitrary transverse dielectric anisotropy," *Proc. Inst. Elec. Eng.*, pt. H, vol. 136, no. 1, pp. 76–79, Feb. 1989.

[11] F. Medina and M. Horno, "Upper and lower bounds on mode capacitances for a large class of anisotropic multilayered microstrip-like transmission lines," *Proc. Inst. Elec. Eng.*, pt. H, vol. 132, no. 3, pp. 157–163, June 1985.

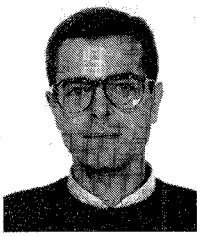

Rafael R. Boix was born in Melilla, Spain, on September 10, 1962. He received the B.Sc. and M.Sc. degrees in physics (Electronics Division) from Seville University, Seville, Spain, in 1985 and 1986 respectively. Currently, he is a Ph.D. student at Seville University, where he is doing research on the analysis of planar lumped elements on anisotropic substrates for MIC and MMIC applications.

✠

Manuel Horno (M'75) was born in Torre del Campo (Jaen), Spain. He received the M.Sc. degree in physics in June 1969 and the Ph.D. degree in physics in January 1972, both from Seville University, Seville, Spain.

Since October 1969 he has been with the Department of Electronics and Electromagnetism at Seville University, where he became an Assistant Professor in 1970, an Associate Professor in 1975, and Professor in 1986. His main fields of interest include boundary value problems in electromagnetic theory, wave propagation in anisotropic media, and microwave integrated circuits. He is presently engaged in the analysis of planar multiconductor transmission lines and lumped elements embedded in anisotropic substrates. He is also interested in the study of planar slow-wave structures, with semiconductor and ferrimagnetic materials.